International Journal of Heat and Mass Transfer 54 (2011) 4875–4884

Contents lists available at ScienceDirect

International Journal of Heat and Mass Transfer

journal homepage: www.elsevier.com/locate/ijhmt

Experimental investigation and numerical analysis for one-stage thermoelectric cooler considering Thomson effect

Chien-Yi Du, Chang-Da Wen *

Department of Mechanical Engineering, National Cheng Kung University, No. 1, University Road, Tainan 701, Taiwan

ARTICLE INFO

Article history:
Received 4 March 2011
Received in revised form 20 June 2011
Accepted 20 June 2011
Available online 23 July 2011

Keywords:
Thermoelectric cooler
Seebeck effect
Peltier effect
Thomson effect
Experiment
Simulation

ABSTRACT

This study conducts experimental investigation and numerical analysis for one-stage thermoelectric cooler (TEC) considering Thomson effect. Three Seebeck coefficient models are applied to numerically and experimentally study the Thomson effect on TEC. Results show that higher current, higher hot side temperature, or lower heat load can increase the temperature difference between the cold and hot sides. Opposite trends are found for COP. Specific current should be chosen as the upper threshold in thermoelectric cooler design. The cooling performance can improve when the Thomson heat maintains positive.

1. Introduction

Development of high density, high power, and high efficiency of electronic components enhances the system efficiency but accompanies with heat dissipation problems. Dramatically increasing heat flux may result in the failure of electronic component or the decrease in efficiency and reliability of system. Therefore, an efficient cooling method is highly desirable to precision electronic components.

Thermoelectric cooler (TEC) is one of the common cooling methods with special features and potential. It can be manufactured from millimeter scale to micrometer scale and even can be made inside the electronic component to do thermal management directly. This suits well for the limited installation space inside electric equipment in practical application. It's an active cooling method, but there is no working fluid and mechanical operation inside. Therefore, its silence and no vibration while working won't cause physical effect on electronic components. Moreover, due to its direct conversion between electrical energy and thermal energy, thermal management is more efficient than other electronic cooling devices and heat can be controlled precisely.

Thermoelectric effects involve the conversion between electrical energy and thermal energy. Three main findings of thermoelectric effects, Seebeck effect, Peltier effect, and Thomson effect, can be traced back to the early 19th century. Seebeck effect was found that in a closed circuit made from two dissimilar metals, there would generate an electrical current with the junctions at different temperatures. Seebeck effect can occur in a circuit composed of any substance, but the magnitude of the Seebeck coefficient is dependent on the material. Peltier effect can be viewed as the inverse effect of Seebeck effect. The heat absorbed is defined as the Peltier heat. Thomson effect was observed that if an electrical current was offered to a single conductor with a temperature difference between two endpoints, material will emit or absorb heat. The combination of Seebeck effect, Peltier effect and Thomson effect is called "Kelvin relationships". A property, "figure-of-merit (Z)", is then defined by scientists to represent characteristics of these three properties. The expression of figure-of-merit is

$$Z = \frac{\alpha^2 \sigma}{k}, \tag{1}$$

where α is Seebeck coefficient, σ is electrical conductivity and k is thermal conductivity.

Theories of thermoelectric effects were fundamentally developed by scientists [1–4]. Chen et al. [5] discussed the influence of Thomson effect on the thermoelectric generator and provided the new relationships considering Thomson effect to express the maximum power output and the maximum efficiency. Yamanashi [6] proposed to optimize the design of the thermoelectric cooler by the dimensionless entropy flow equations. Chua et al. [7] studied the relationship between temperature and entropy. The entropy density was applied to explain the capacity of thermoelectric cooling and thermoelectric generation. Xuan et al. [8–13] adopted fundamental thermodynamics and temperature–entropy diagrams to

* Corresponding author. Tel.: +886 6 2757575x62110; fax: +886 6 2352973.
E-mail address: alexwen@mail.ncku.edu.tw (C.-D. Wen).

0017-9310/$ - see front matter © 2011 Elsevier Ltd. All rights reserved.
doi:10.1016/j.ijheatmasstransfer.2011.06.043

Nomenclature

A_p	cross section area of one semiconductor pellet
COP	coefficient of performance
CSM	constant Seebeck coefficient model
i	variable
I	current
J	current density
LLS	log-linear Seebeck coefficient model
LSM	linear Seebeck coefficient model
L_x	length of one semiconductor pellet
N	number of P–N pair
P_{TEC}	thermoelectric cooler power
Q_c	cold side heat load
Q_u	hot side heat load
R^2	coefficient of determination
T	temperature
T_c	cold side temperature
T_u	hot side temperature
V_{TEC}	thermoelectric cooler voltage
X	the x-axis in Cartesian coordinate system
Z	Figure of merit
ΔT	temperature difference between hot side and cold side

Greek symbols

α	Seebeck coefficient
κ	heat conductivity
μ_τ	Thomson heat
ρ	electrical resistivity
σ	electrical conductivity
τ	Thomson coefficient

Subscripts

c	cold side
max	maximum
opt	optimum
rev	reverse
tau	positive Thomson heat
TEC	thermoelectric cooler
u	hot side
x	x-direction

analyze the internal heat distribution of thermoelectric cooler at steady state and when the interface layer is considered. Multi-stage thermoelectric coolers were further investigated and the polar characteristics of the coefficient of performance were used to optimize the design. Yang and Chen [14] analyzed the cooling capacity of one- and two-stage thermoelectric microcoolers without considering Thomson effect and pointed that the techniques of integrated circuit and microelectromechanical manufacturing are two primary skills for thermoelectric cooling development. Chen et al. [15] applied thermoelectric cooler to high power light-emitting diode (LED) by microfabrication technique and flip-chip assembly process, and analyzed the effect of varied semiconductor pairs on decreasing the internal heat resistivity of LED. Hodes [16] simulated one-dimensional temperature distribution of thermoelectric modules. Different from most previous investigations, the controlled side and uncontrolled side were defined as boundary conditions. The controlled side had three operating forms with varied current supplied: cooling, heating and neutral forms. Huang et al. [17] studied the influence of Thomson effect by simulating the temperature distribution and coefficient of performance of one-stage thermoelectric cooler with known cold side and hot side temperatures. Results showed that Thomson heat could lower the effect of Joule heat at the cold side. The methods to improve the coefficient of performance should consider not only a better figure-of-merit but also the influence of Thomson effect. Kraftmakher [18] proposed how to measure the Seebeck coefficient and the Peltier coefficient of thermoelectric cooler with simple experimental methods. Lee and Kim [19] conducted three-dimensional numerical analysis o predict the optimal performance for thermoelectric micro-cooler. Results showed that the performance of thermoelectric cooler can be improved more for thick thermoelectric elements at small temperature difference and small current. The key factors to evaluate the performance of the thermoelectric microcooler were more pairs of semiconductor or smaller cross-sectional area of semiconductor. Chang et al. [20] established a theoretical model of the thermal analogy network for thermoelectric air-cooling module. The influence of thermal resistances was analyzed and the appropriate operating range was predicted. Yamashita [21] investigated the resultant Seebeck coefficient which is derived from the temperature dependence of the intrinsic Seebeck coefficient by considering the Thomson effect. It is found that both the resultant Seebeck coefficient and the resultant figure-of-merit were larger than the intrinsic properties and the figure-of-merit was affected dramatically at the interfaces when the intrinsic Seebeck coefficient varied nonlinearly with temperature. Pichanusakorn and Bandaru [22] maximized the power factor ($\alpha^2\sigma$) to find the optimal Seebeck coefficient. Results showed that for any material, the maximum power factor at a given temperature is expected when the Seebeck coefficient in the range of 130–187 μV/K.

In previous investigations of thermoelectric cooler, constant hot and cold side temperatures of thermoelectric module were often chosen as boundary conditions. However, like Hodes [16], the hot side temperature and the cold side heat load are controlled in this study. The cold side heat load is controlled in order to meet the known allowable power input for the electronic components in practical application. The hot side temperature of thermoelectric module remains fixed to easily observe the cold side temperature variation. Therefore, with a variety of input current, the heat load of the cold side, and the hot side temperature controlled by the blower system, the cold side temperature and the coefficient of performance of one-stage thermoelectric cooler are obtained through the experiment and numerical simulation.

On the other hand, not only Joule heat but also Thomson heat is taken into account in the internal thermal analysis of thermoelectric cooler. In order to discuss the effect of Thomson heat on temperature prediction and the interior heat transfer mechanism, three different Seebeck coefficient models, constant Seebeck model (CSM), second-order linear Seebeck model (LSM), and first-order log-linear Seebeck model (LLS), are examined through experimental investigation and numerical simulation. CSM indicates a zero Thomson coefficient. LSM means the Thomson coefficient is a function of temperature, LLS represents a constant Thomson coefficient. The best Seebeck coefficient model is determined by comparing simulation results with experimental results. Thermal analysis considering Thomson heat is then simulated with the best Seebeck model, and the influence of Thomson heat, Fourier heat and Joule heat on one-stage thermoelectric cooler is analyzed.

2. General model of one-stage thermoelectric cooler

A thermoelectric cooler is composed of several semiconductor pairs which are sandwiched between two ceramic layers, as shown

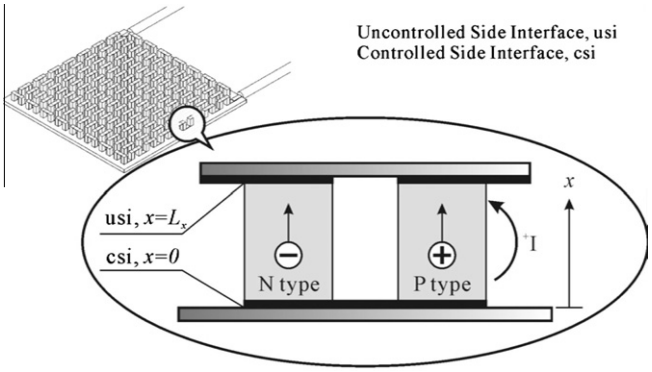

Fig. 1. Schematic diagram of one pair of semiconductors.

in Fig. 1. A pair of semiconductors in thermoelectric cooler is chosen as the micro-system for analysis. The x-axis of the thermoelectric cooler is defined positive from down side to upper side, i.e. the flowing direction of current in p-type is positive. The down side where the heat absorption occurs is controlled side, the cold side of thermoelectric cooler. The upper side where the heat release occurs is uncontrolled side, the hot side of thermoelectric cooler. Properties of p-type and n-type are assumed to be equal except the Seebeck coefficient and electric current are negative in n-type. Thus the temperature distributions in p-type and in n-type are the same. Governing equation of one-stage thermoelectric cooler is derived according to irreversible thermodynamics, thermoelectric relations and Onsager's Reciprocal Relations [1–4]. One can obtain the three-dimensional governing equation

$$k\nabla^2 T - \tau J \cdot \nabla T + \rho J^2 = 0, \tag{2}$$

where k is thermal conductivity, τ is Thomson coefficient, J is defined as the electric current density, and electrical resistivity ρ is the reciprocal of electrical conductivity ($\rho = 1/\sigma$). The first term is the heat resulted from Fourier conduction, the second term and the last term are attributed to heat generation from the Thomson heat (μ_τ) and the Joule heat.Different from previous investigations using constant hot and cold side temperatures as boundary conditions, the hot side temperature (T_u) and the cold side heat load (Q_c) are controlled in this study. The boundary equations are

$$T|_{x=L_x} = T_u, \tag{3}$$

$$Q|_{x=0} = Q_c. \tag{4}$$

The heat balance at the hot side boundary is

$$Q_u = 2NI\alpha|_{x=L_x} T_u - 2N\kappa A_p \frac{dT}{dx}|_{x=L_x}, \tag{5}$$

where N is the number of pair of semiconductors; A_p is the cross-sectional area of p-type semiconductor. The first term indicates the heat resulted from Peltier cooling effect and the second term is from the Fourier conduction. The total power of one-stage thermoelectric cooler can be obtained from the heat loads,

$$P_{\mathrm{TEC}} = Q_u - Q_c = 2NI\alpha|_{x=L_x} T_u - 2N\kappa A_p \left.\frac{dT}{dx}\right|_{x=L_x} - Q_c. \tag{6}$$

Therefore, the input voltage of one-stage thermoelectric cooler is

$$V_{\mathrm{TEC}} = 2N\alpha|_{x=L_x} T_u - 2N\frac{\kappa}{J}\left.\frac{dT}{dx}\right|_{x=L_x} - \frac{Q_c}{I}. \tag{7}$$

Finally, the coefficient of performance (COP) of test module is defined as the cooling rate per unit power input of test module,

$$\mathrm{COP} = \frac{Q_c}{P_{\mathrm{TEC}}} = \frac{Q_c}{2NI\alpha|_{x=L_x} T|_{x=L_x} - 2N\kappa A_p \frac{dT}{dx}|_{x=L_x} - Q_c}. \tag{8}$$

Only when $\Delta T > 0$, COP has significance.

3. Numerical methods

In this study Thomson heat (μ_τ) is taken into account in order to discuss its effect on temperature prediction and the internal heat transfer mechanism of one-stage thermoelectric cooler. Thomson heat and Thomson coefficient (τ) can be determined by the Seebeck coefficient. Therefore, three different Seebeck coefficient models, constant Seebeck model (CSM), second-order linear Seebeck model (LSM), and first-order log-linear Seebeck model (LLS), are examined for suitability and accuracy. The mathematical forms of these three models are listed in Table 1. In CSM model, Seebeck coefficient is a constant property, which is mostly used in thermoelectric cooler analysis. The constant Seebeck coefficient leads to a zero Thomson Coefficient, i.e. the Thomson effect is neglected. LSM model and LLS model are both temperature-dependent. LSM model indicates that both Seebeck coefficient and Thomson coefficient are the function of temperature. LLS model has a constant Thomson coefficient. The coefficients C_0, C_1 and C_2 in these three models are determined through experiment.

Several assumptions are made to simplify the simulation: (1) The test module operates in steady state, and all properties are independent of time; (2) Electric current flows along single direction without scattering; (3) Energy only transmits across the cold side and the hot side of the test module. The other parts are assumed to be in adiabatic condition, i.e. no energy transfer; (4) Heat only flows along the x-direction; (5) Heat load supplied by heating unit is completely absorbed by the test module; (6) Thermal conductivity and electrical resistivity are viewed as constants at any temperature, and their values are obtained from the average value of measurement; (8) Seebeck coefficient at different temperatures is measured in experiment. The data of Seebeck coefficient will be applied to determine CSM model, LSM model and LLS model; (9) The properties of p-type are equal to the properties of n-type. Only the electric current and the Seebeck coefficient are negative in n-type.

3.1. Second-order linear Seebeck model (LSM)

Second-order LSM model represents that the Thomson coefficient is a second-order polynomial. Hence the governing equation becomes a non-linear ordinary differential equation

$$\frac{d^2T}{dx^2} - \frac{J}{\kappa}(2C_2T^2 + C_1T)\frac{dT}{dx} + \frac{J^2\rho}{\kappa} = 0. \tag{9}$$

The governing equation is then resolved numerically

$$\frac{d^2T^{(t+1)}}{dx^2} - \frac{J}{\kappa}(2C_2T^2 + C_1T)^{(t)}\frac{dT^{(t+1)}}{dx} + \frac{J^2\rho}{\kappa} = 0, \tag{10}$$

where the superscript (t) indicates the old value; $(t+1)$ means the new value.Eq. (10) is rewritten with finite difference method,

Table 1
Mathematical form of Seebeck coefficient models in this study.

Seebeck models	Formula
2nd-order LSM	$\alpha = C_0 + C_1T + C_2T^2$
CSM	$\alpha = C_0$
1st-order LLS	$\alpha = C_0 + C_1 \ln T$

$$\left(\frac{T_{i+1}-2T_i+T_{i-1}}{\Delta x^2}\right)^{(t+1)} - \frac{J}{\kappa}\left[2C_2(T^{(t)})^2+C_1T^{(t)}\right]\left(\frac{T_{i+1}-T_{i-1}}{2\Delta x}\right)^{(t+1)}+\frac{J^2\rho}{\kappa} = 0. \quad (11)$$

Eq. (11) is rearranged,

$$-\frac{J^2\rho\Delta x^2}{\kappa} = \{1-\frac{J}{2\kappa}\Delta x[2C_2(T^{(t)})^2+C_1T^{(t)}]\}T_{i+1}^{(t+1)} - 2T_i^{(t+1)} + \{1+\frac{J}{2\kappa}\Delta x[2C_2(T^{(t)})^2+C_1T^{(t)}]\}T_{i-1}^{(t+1)}. \quad (12)$$

The heat balance at the cold side boundary is

$$Q_c = 2NI\alpha|_{x=0}T|_{x=0} - 2N\kappa A_p\left.\frac{dT}{dx}\right|_{x=0}, \quad (13)$$

$$\frac{Q_c}{2NI} = [C_0+C_1T(0)+C_2T(0)^2]T_i - \frac{\kappa}{J}\left(\frac{-3T_i+4T_{i+1}-T_{i+2}}{2\Delta x}\right). \quad (14)$$

Therefore, Eq. (14) is rewritten in the form of point solution,

$$T_i^{(t+1)} = \frac{\frac{Q_c}{2NI}+\frac{\kappa}{2\Delta xJ}(4T_{i+1}^{(t)}-T_{i+2}^{(t)})}{C_0+C_1T_i^{(t)}+C_2(T_i^{(t)})^2+\frac{3\kappa}{2\Delta xJ}}. \quad (15)$$

3.2. Constant Seebeck model (CSM)

Thomson coefficient (τ) is zero in CSM. The governing equation is

$$\frac{d^2T}{dx^2}+\frac{J^2\rho}{\kappa} = 0. \quad (16)$$

The equation turns into a second-order linear ordinary differential equation and can be solved analytically.

3.3. First-order log-linear Seebeck model (LSM)

The characteristic in 1st-order LSM is that Thomson coefficient is a constant in this model. Then the governing equation is rewritten as

$$\frac{d^2T}{dx^2}-C_1\frac{J}{\kappa}\frac{dT}{dx}+\frac{J^2\rho}{\kappa} = 0. \quad (17)$$

The governing equation also becomes a linear problem. Therefore, it can be either solved analytically like CSM model or numerically like LSM model.

4. Experimental methods

4.1. Test facility

As shown in Fig. 2, the main components of the test apparatus consist of test section, power supply, data acquisition system, and surroundings control system. The linear DC power supply made by the Good Will Instrument Co. Ltd. provides the required voltage and current for test section and the forced convection section in surroundings control system.

Fig. 3 shows the detailed construction of the test section. It mainly includes test module, heat sink unit, cerablanket, and heating unit. The test module is composed of one thermoelectric cooler and two heat spreaders. Thermoelectric cooler is TEC1-127.08, made by Tande Energy and Temperature Associates Pty. Co. Thickness is 3.8 mm, working area is 40 mm^2, and the operation current range is 0–8 A. The thermoelectric cooler is constructed from 125 pairs of semiconductors and two interface layers. The semiconductor material is Bismuth Telluride (BiTe). Height is about 2 mm and cross-sectional area is 1.4 mm^2. The two 0.9 mm^2 Alumina ceramic interface layers (Al_2O_3) are thermally conductive but electrically insulated. Bismuth Tin (BiSn) is used to connect the interface layer and semiconductors. In between semiconductors, there is silicone, RTV filled to prevent from vapor. The heat spreader is used to distribute the heat uniformly. It is made of brass which has high thermal conductivity and is tractable and dysoxidizable. Three grooves are machined on the spreader to set the thermocouples without destroying the surface of thermoelectric coolers. The insulating blanket (cerablanket) made by Thermal Ceramic Inc. is made of ceramic fiber materials, like silica (SiO_2) and Aluminum oxide (Al_2O_3). It has very low thermal conductivity about 0.07 W/m K below 200 °C to assure the adiabatic condition around the test module. The fins are used as the heat sink and assembled at the top of test module. Totally 144 fins with 1.45 mm^2 rectangle cross-sectional area and 45.5 mm height are made of Al 6063 in one work piece and are uniformly set on the base plate with 45 mm^2 area and 4.5 mm height. A thin silicon rubber heater (40 mm^2) is used as the heating element to meet the known heat load of electronic component in practice. Since the electrical resistance of the heater is fixed, the heat load is then controlled by the input current. In addition, a complementary heater is used to make sure that the heat will not dissipate from the bottom. All junctions between components are filled with thermal compound, Arctic Silver 5 type, made by Arctic Silver Incorporated Company. The average particle size of the thermal compound is small enough to fill the cavities at the contact surfaces in order to reduce the contact thermal resistance.

The data acquisition system includes thermocouple, data acquisition equipment (DAQ) and personal computer. The type T thermocouple is used to measure the hot side temperature and cold side temperature of the test module. The data acquisition equipment, NetDAQ 2640A, made by Fluke Corporation Company includes a universal input module with 20 analog channels, 10 computed channels and 8 alarm channels. It can measure DC and AC voltage, resistance and temperature.

As shown in Fig. 4, surroundings control system composed of fan, wind tunnel, thermostat, and settling chamber is utilized to maintain the desired hot side temperature of test module. The fan drives the air to flow along the wind tunnel and passes through the fin at the top of test section to take the heat away from the test section. The settling chamber made of a porous aluminum board is installed at the entrance of the wind tunnel in order to assure that the air can flow more stably. The thermostat controls the air properties.

4.2. Experimental procedure

Experiments are divided into pre-experiment and main experiment. Three important properties of thermoelectric cooler, thermal conductivity, electrical resistivity and Seebeck coefficient, are measured in pre-experiment. The hot side temperature, cold side temperature, voltage and current of one-stage thermoelectric cooler are measured in main experiment.

In pre-experiment, there is no need to supply current to the thermoelectric cooler. The temperature difference of the thermoelectric cooler is measured with a given heat load. One-dimensional heat conduction is assumed and the thermal conductivity at different temperatures can be calculated by Fourier's law. The electrical resistance is measured at different temperatures. By controlling the temperature difference at 2.5 K ± 0.3 K, the voltage generating by the temperature difference is measured at different temperatures. The Seebeck coefficient is then determined by the ratio of the voltage and the temperature difference.

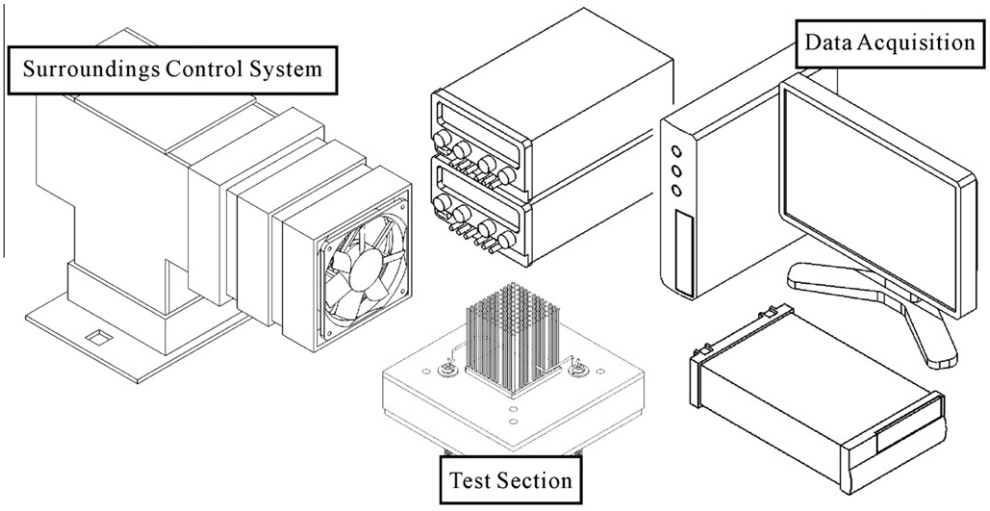

Fig. 2. Experimental facility.

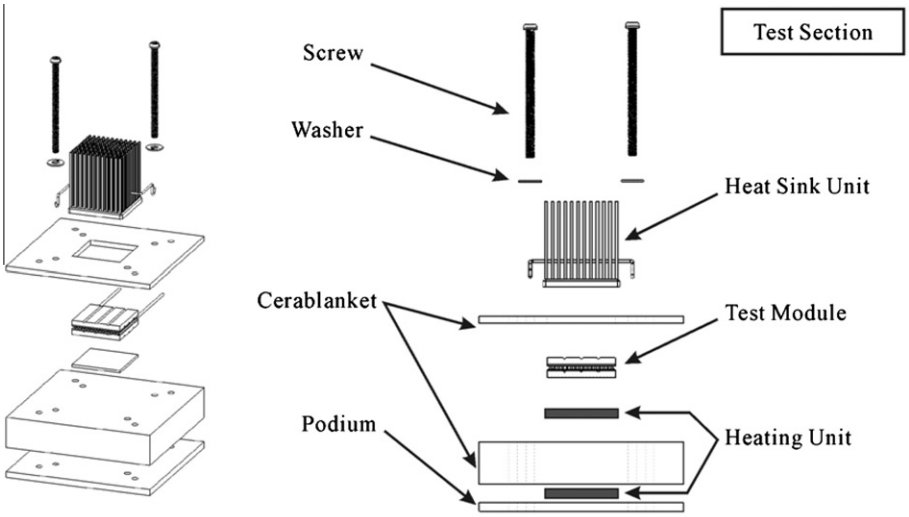

Fig. 3. Construction of test section.

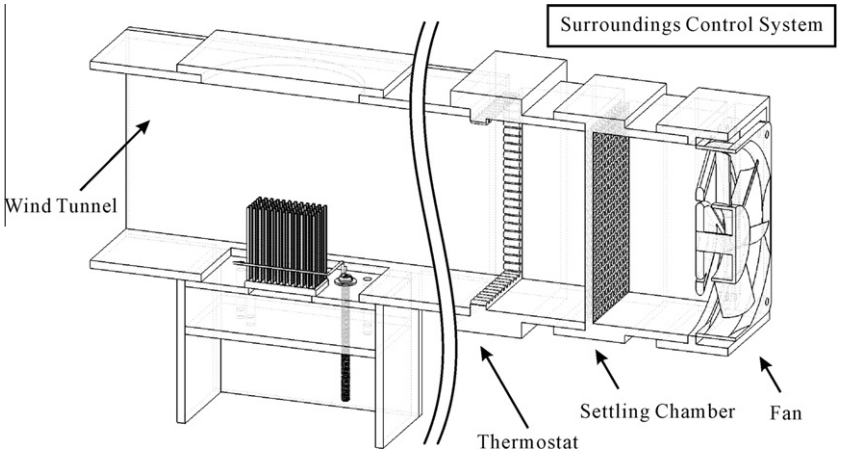

Fig. 4. Construction of surroundings control system.

In main experiment, three hot side temperatures, 323.2 K, 333.2 K, and 343.2 K are selected. Three input heat loads, 5.5 W, 12.3 W and 22.0 W are determined by the input current of heating element with 0.5 A, 0.75 A and 1.0 A. Seven input currents of test

module, 1.0 A, 1.5 A, 2.0 A, 2.5 A, 3.0 A, 3.5 A and 4.0 A are examined. The cold side heat load is controlled by the heating element whose current is supplied by the power supply. The hot side temperature is controlled by the forced convection section. Once the change of the hot side temperature is in ±0.6 K during 900 s, it reaches steady state. The cold side temperature and the voltage of test module are then collected and stored.

5. Results and discussion

5.1. Properties of thermoelectric cooler

Thermal conductivity and electrical resistivity of single thermoelectric cooler are first measured at different temperatures. Results show that thermal conductivity decreases but electrical resistivity increases with increasing temperature. However, both changes are small enough to be neglected. Thus thermal conductivity and electrical resistivity can be assumed constant. The properties of thermoelectric cooler are listed in Table 2.

Fig. 5 shows Seebeck coefficient is a function of temperature and increases with increasing temperature. Three Seebeck coefficient models (CSM, LSM and LLS) are examined for suitability and accuracy. The average value of all measured data is used as the constant Seebeck coefficient in CSM model. The formulas of LSM model and LLS model are obtained by regression. On the other hand, Thomson coefficient is defined as

$$\tau = T\frac{d\alpha}{dT}. \tag{18}$$

Fig. 6 shows the Thomson coefficient for three models. CSM model leads to a zero, LSM model is temperature-dependent, and LLS model has a constant value.

5.2. Experimental results

For one-stage thermoelectric cooler with fixed hot side temperature (T_u) and the fixed cold side heat load (Q_c), the temperature difference (ΔT) and COP are obtained by changing the input current of test module (I). Fig. 7 shows the distributions of temperature difference with increasing current for different T_u and different Q_c. Due to the insufficiency of the surroundings control system when a low current and a high cold side heat load are applied, the desired hot side temperature cannot be attained so that there is no measured data. Results show that temperature difference increases with increasing current. Since the hot side temperature is fixed, this means the cold side temperature goes down with increasing current. At the same current, temperature difference decreases with increasing heat load. It is observed that the slope of temperature difference decreases with increasing current and is expected to approximate to zero at a specific current which means there will exist a maximum temperature difference. Regarding the effect of hot side temperature, overall the trends are found similar. To emphasize the difference in magnitude, Fig. 8 shows the distributions of temperature difference with increasing current for different T_u at Q_c = 12.3 W. At the same current, temperature difference slightly increases with increasing hot side temperature. However, comparing with the effect of heat load, the change of temperature difference resulted from the different hot side temperature is minor.

Table 2
Properties of one-stage TEC in this study.

Properties	Values
Number of P–N pair (N)	125
Length of one semiconductor pellet (L_x)	2.0×10^{-3} m
Cross-sectional area of one semiconductor pellet (A_p)	1.96×10^{-6} m^2
Thermal conductivity of one semiconductor pellet (κ)	2.571 W m^{-1} K^{-1}
Electrical resistance of one semiconductor pellet (R)	1.80 Ω
Electrical resistivity of one semiconductor pellet (ρ)	7.056×10^{-6} Ω m

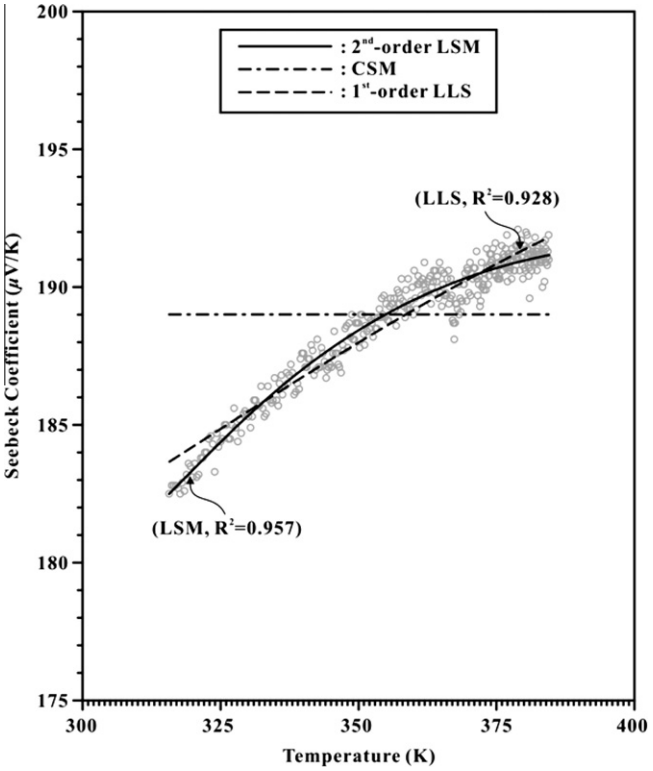

Fig. 5. Comparison of three Seebeck coefficient models.

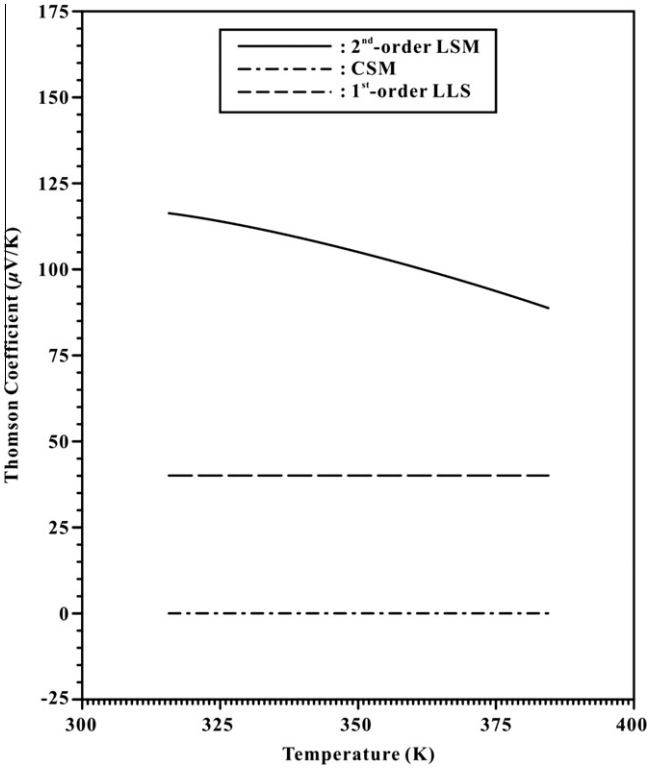

Fig. 6. Comparison of Thomson coefficient with different Seebeck coefficient models.

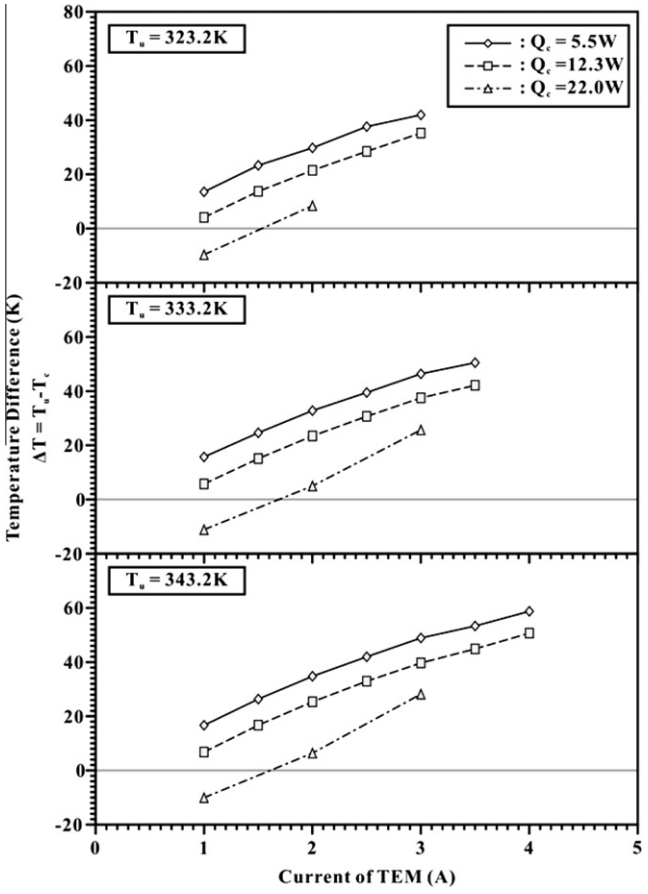

Fig. 7. Temperature difference at different hot side temperatures with different cold side heat loads.

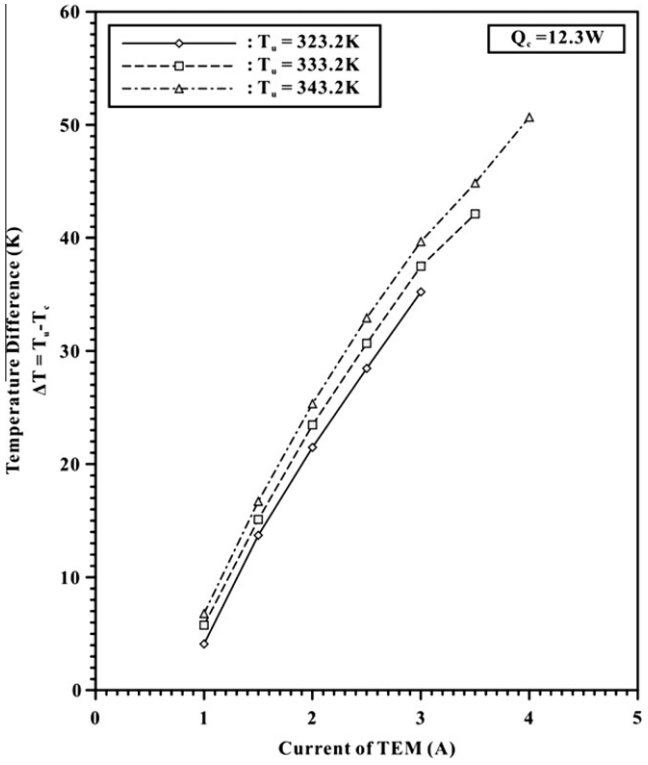

Fig. 8. The variations of temperature difference at different hot side temperatures with the cold side heat load 12.3 W.

Fig. 9 shows the distributions of COP with increasing current for different T_u with different Q_c. The COP has no meaning when the test module loses its cooling capacity ($\Delta T < 0$). Therefore, the meaningless data will not be shown in the figure. The trend of COP is opposites to that of ΔT, the COP decreases with increasing current. According to the definition of COP, Eq. (8), the COP decreases when increasing the current of test module with a fixed cold side heat load. Moreover, the COP decreases quickly at higher current and almost approximates to zero. The maximum COP appears when the TEC current is small enough to make the temperature differences approximate to zero. With fixed current, adding heat load makes COP larger and temperature difference smaller. Fig. 10 shows the difference of hot side temperature has relatively small effect on COP and can almost be neglected.

5.3. Numerical simulation

Higher current values are examined in order to find the maximum temperature difference in numerical simulation. Thomson heat is taken into account in order to discuss its effect on the internal temperature prediction and heat transfer mechanism for one-stage thermoelectric cooler.

In Fig. 11, the temperature differences for three different Seebeck models are simulated at the hot side temperature 343.2 K with the cold side heat load 12.3 W. Results show that there does exist a maximum temperature difference (ΔT_{max}) for each model at a specific current which is defined as the optimum current, I_{opt}. Larger than this current, the heat generation will generate faster than the Peltier cooling heat, so the temperature difference starts

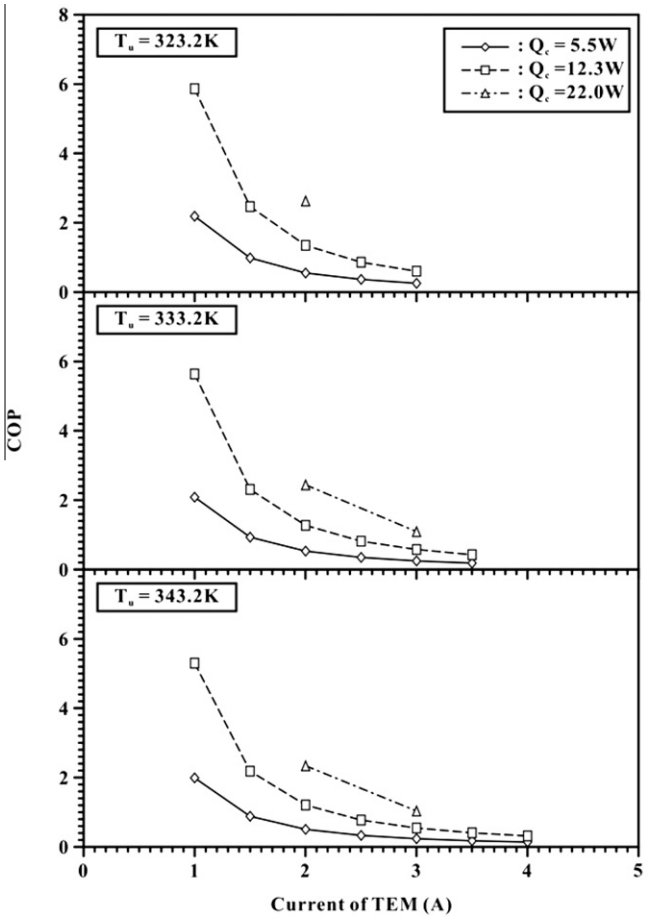

Fig. 9. COP at different hot side temperatures with different cold side heat loads.

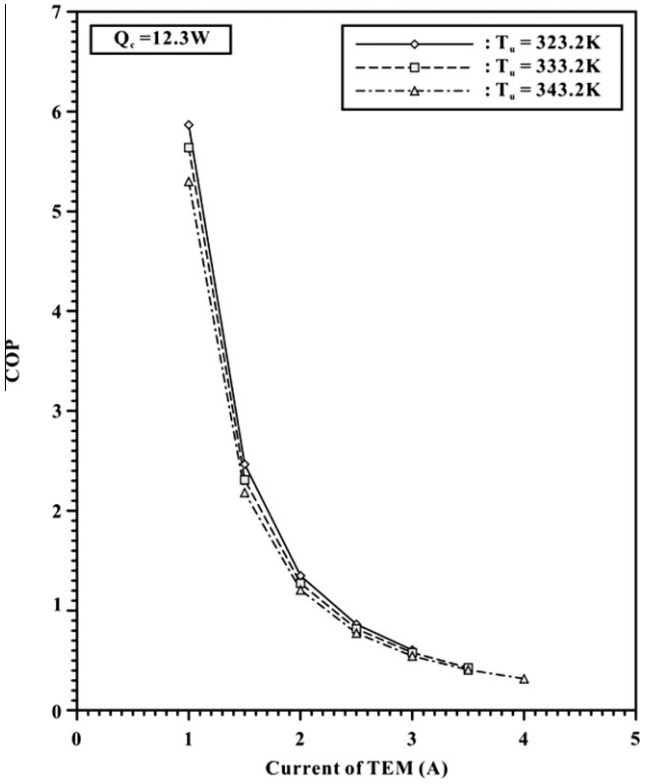

Fig. 10. The variations of COP at different hot side temperatures with the cold side heat load 12.3 W.

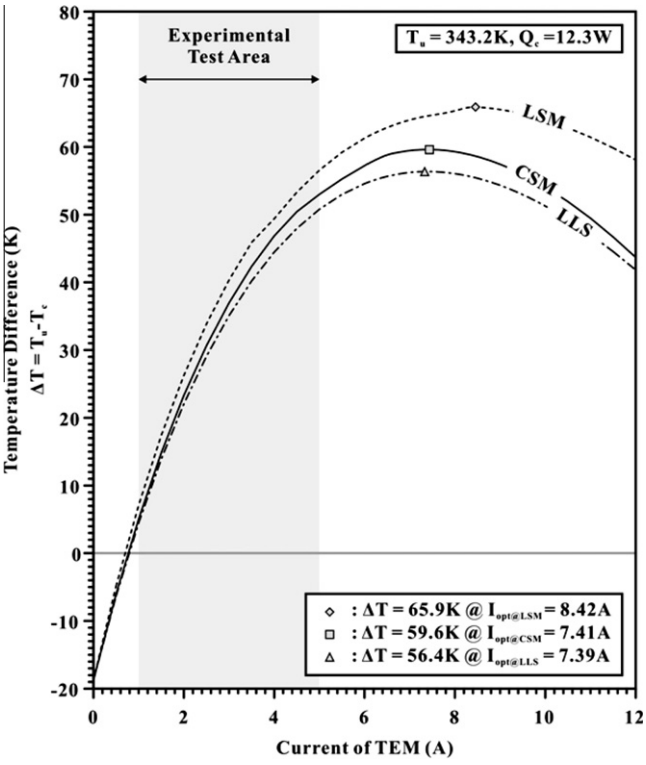

Fig. 11. Comparison of temperature difference simulated by CSM model, LSM model and LLS model.

to decrease. Therefore, in thermoelectric cooler design the input current must be smaller than the optimal current in order to achieve cooling. In addition, the effect of Seebeck model becomes apparent at higher current range. It is necessary to examine their suitability and accuracy while being applied in simulation.

Figs. 12 and 13 show the comparison of numerical results and experimental data for temperature difference and COP at the hot side temperature 343.2 K with the cold side heat load 12.3 W. From the figures, LSM model shows the best agreement with the experimental data, CSM model in second, and LLS model in last. In LSM model, the Seebeck coefficient and the Thomson coefficient are both dependent on temperature. The poor results of LLS model may be due to the over-predicting by constant Thomson coefficient. Overall, LSM model is found to be the best Seebeck coefficient model in this study.

The internal temperature prediction and heat transfer mechanism for one-stage thermoelectric cooler is simulated with the best Seebeck model, LSM model. At a given hot side temperature 333.2 K with the cold side heat load 12.3 W, the internal temperature distributions with current change (0–12 A) is shown in Fig. 14. When the current is zero, only Fourier conduction occurs so that the temperature at the cold side near the heat source is higher than the hot side temperature near surroundings. Thermoelectric effects occur after providing the current into the test module and cause the drop of cold side temperature. The internal temperature will be larger than the hot side temperature beyond a specific current which is defined as reverse current, I_{rev}, where the positive temperature gradient at the hot side starts to turn into negative. The heat generation inside will increase faster than the cooling from the hot side. Therefore, for practical use, input current should be lower than I_{rev} to prevent from high internal temperature which may result in the failure of test module. As defined earlier, the optimum current, I_{opt}, will cause the maximum temperature difference, i.e. the cold side temperature is the lowest. According to the results,

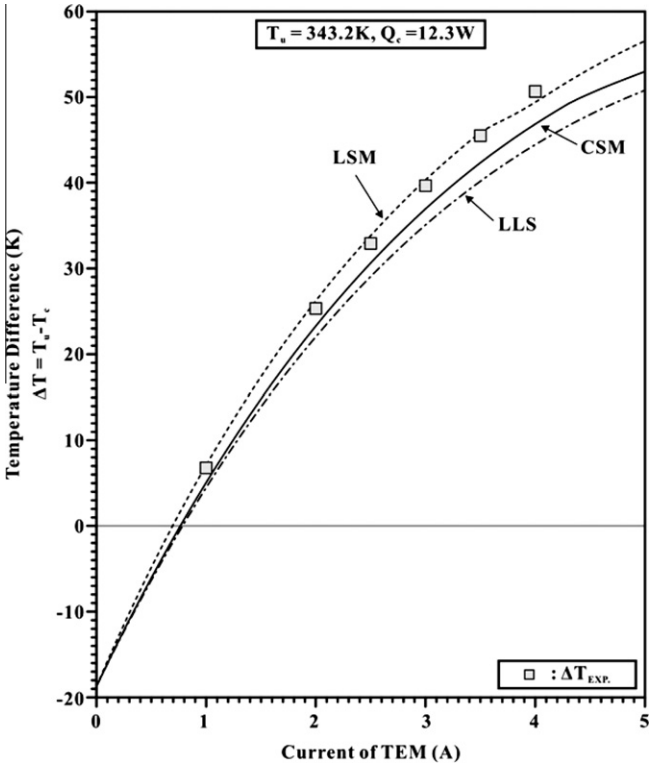

Fig. 12. Comparison of temperature difference simulated by three Seebeck coefficient models at the hot side temperature 343.2 K with the cold side heat load 12.3 W.

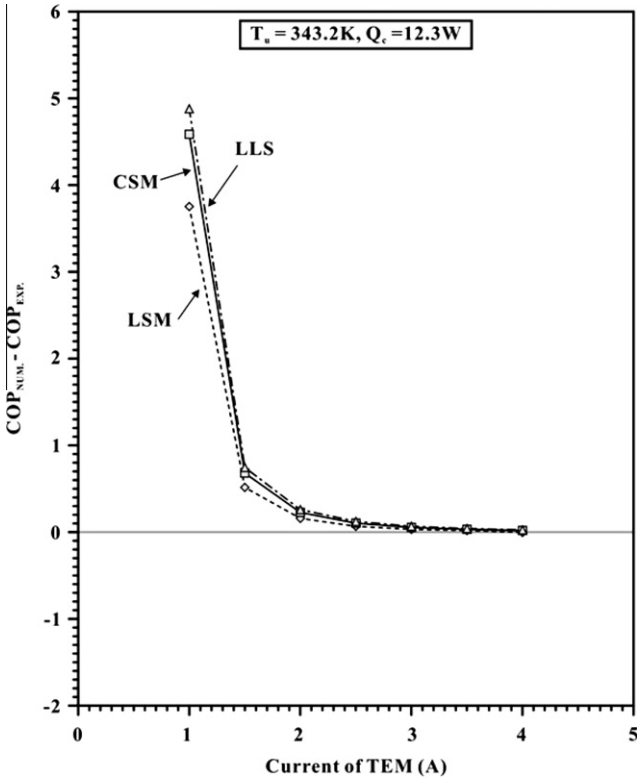

Fig. 13. Comparison of COP simulated by three Seebeck coefficient models at the hot side temperature 343.2 K with the cold side heat load 12.3 W.

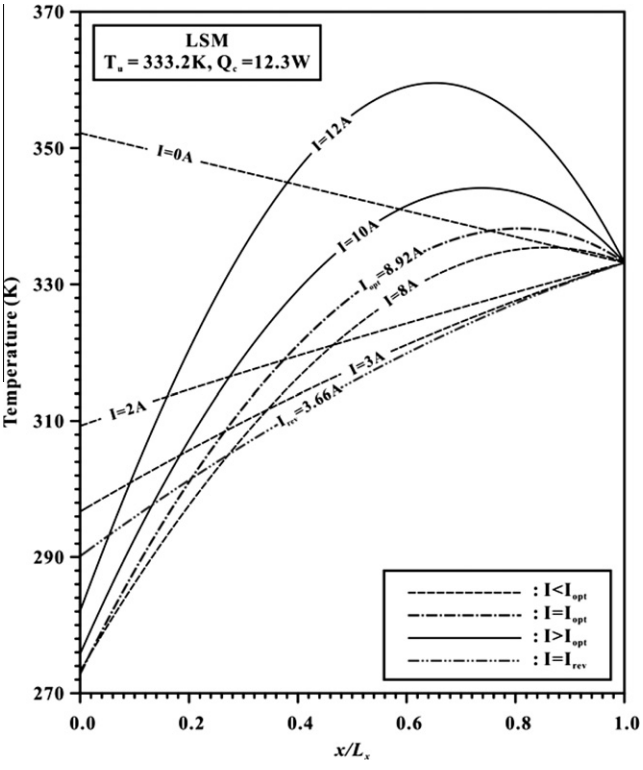

Fig. 14. The internal temperature distribution versus different currents at the hot side temperature 333.2 K with the cold side heat load 12.3 W using LSM model.

I_{opt} = 8.92 A and I_{rev} = 3.66 A, I_{rev} should be chosen as the upper threshold in thermoelectric cooler design.

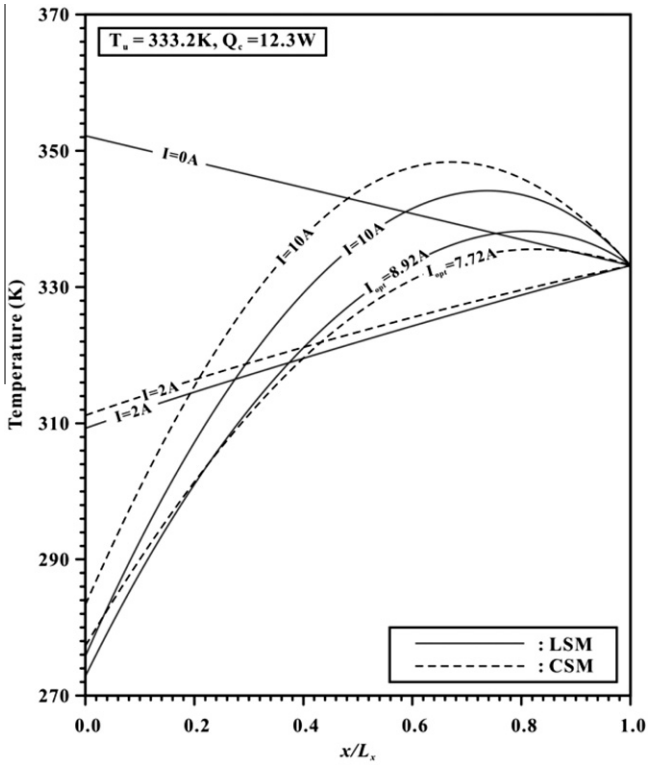

Fig. 15. Comparison of internal temperature distribution between LSM model and CSM model.

The internal temperature distribution of LSM model considering Thomson heat and CSM model neglecting Thomson heat is shown

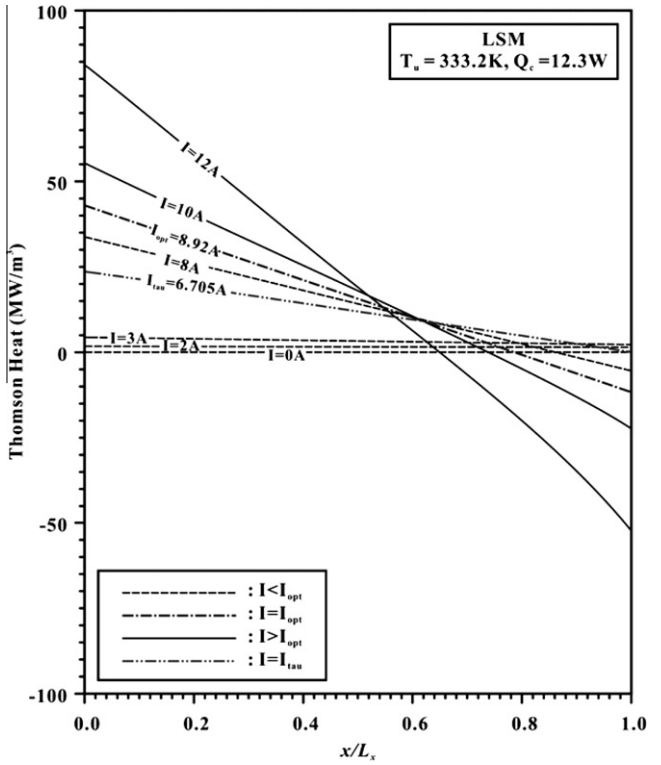

Fig. 16. Distribution of Thomson heat at the hot side temperature 333.2 K and with the cold side heat load 12.3 W using LSM model.

in Fig. 15. As discussed earlier, the cold side temperature prediction in LSM model is better than in CSM model by comparing with experimental data. Results here show the temperature simulated in LSM model is obviously lower than in CSM model. This indicates that applying the CSM model is a more conservative method to estimate the maximum temperature difference of TEC, while the actual temperature difference is larger in application.

The internal thermal mechanism includes Fourier heat conduction, Joule heat and Thomson heat. The sum of Thomson heat and Joule heat plays the role of heat generation inside TEC. The distribution of Thomson heat is shown in Fig. 16. When the Thomson heat is positive, it plays the role of cooling in the interior to reduce the effect of Joule heat and Fourier conduction and enhance the cooling capacity of the TEC. If the Thomson heat at any position inside turns into negative, where the current is defined as I_{tau}, the Thomson heat becomes part of the heat generation and causes the internal temperature to rise quickly. Therefore, the cooling performance can improve when the Thomson heat maintains positive. Comparing the value of Joule heat and Thomson heat, Joule heat is larger than Thomson heat. Hence the Joule heat dominates in the internal thermal mechanism, but there is a need to achieve more precise temperature control by considering Thomson heat.

6. Conclusions

The purpose of this research is to analyze the performance of one-stage thermoelectric coolers by experiment and numerical simulation. The influence of Thomson effect is also discussed. Key findings from the study are summarized below.

1. Temperature difference increases with increasing current and decreases with increasing heat load. Temperature difference slightly increases with increasing hot side temperature, but the effect of hot side temperature is minor.
2. COP decreases with increasing current and approximates to zero at a high current. The maximum COP appears when the TEC current is small enough to make the temperature differences approximate to zero. Adding heat load makes COP larger and temperature difference smaller. The hot side temperature has relatively small effect on COP and can almost be neglected.
3. There exists a maximum temperature difference at high current. The effect of Seebeck model becomes apparent at higher current range. It's necessary to examine their suitability and accuracy while being applied in simulation. Overall, LSM model is found to be the best Seebeck coefficient model.
4. The internal temperature will be larger than the hot side temperature beyond the reverse current, I_{rev}. The heat generation inside will increase faster than the cooling from the hot side. Therefore, I_{rev} should be chosen as the upper threshold in thermoelectric cooler design to prevent from high internal temperature which may result in the failure of test module.
5. Applying the CSM model is a more conservative method to estimate the maximum temperature difference of TEC. Actually the temperature difference is larger in application.
6. The cooling performance can improve when the Thomson heat maintains positive. Joule heat dominates in the internal thermal mechanism, but more precise temperature control can be achieved by considering Thomson heat.

Acknowledgment

The authors are grateful for the support of the National Science Council of Taiwan (with Project No. NSC 98-2221-E-006-172).

References

[1] L. Onsager, Reciprocal relations is irreversible processes. I, Phys. Rev. 37 (1931) 405–426.
[2] H.B. Callen, The application of Onsager's reciprocal relations to thermoelectric, thermomagnetic, and galvanomagnetic effects, Phys. Rev. 73 (1948) 1349–1358.
[3] C.A. Domenicali, Irreversible thermodynamics of thermoelectric effects in inhomogeneous, anisotropic media, Phys. Rev. 92 (1953) 877–881.
[4] Abram Fedorovich Ioffe, Semiconductor Thermoelements, and Thermoelectric Cooling, Infosearch, Ltd., London, 1957.
[5] J. Chen, Z. Yan, L. Wu, The influence of Thomson effect on the maximum power output and maximum efficiency of a thermoelectric generator, J. Appl. Phys. 79 (11) (1996) 8823–8828.
[6] M. Yamanashi, A new approach to optimum design in thermoelectric cooling systems, J. Appl. Phys. 80 (9) (1996) 5494–5502.
[7] H.T. Chua, K.C. Ng, X.C. Xuan, C. Yap, J.M. Gordon, Temperature–entropy formulation of thermoelectric thermodynamic cycles, Phys. Rev. E 65 (2002) 056111.
[8] X.C. Xuan, K.C. Ng, C. Yap, H.T. Chua, A general model for studying effects of interface layers on thermoelectric devices performance, Int. J. Heat Mass Transfer 45 (2002) 5159–5170.
[9] X.C. Xuan, Analyses of the performance and polar characteristics of two-stage thermoelectric coolers, Semicond. Sci. Technol. 17 (2002) 414–420.
[10] X.C. Xuan, On the optimal design of multistage thermoelectric coolers, Semicond. Sci. Technol. 17 (2002) 625–629.
[11] X.C. Xuan, Optimum design of a thermoelectric device, Semicond. Sci. Technol. 17 (2002) 114–119.
[12] X.C. Xuan, K.C. Ng, C. Yap, H.T. Chua, The maximum temperature difference and polar characteristic of two-stage thermoelectric coolers, Cryogenics 42 (2002) 273–278.
[13] X.C. Xuan, K.C. Ng, C. Yap, H.T. Chua, Temperature-entropy diagrams for multistage thermoelectric coolers, Semicond. Sci. Technol. 18 (2003) 273–277.
[14] R. Yang, G. Chen, Multistage thermoelectric microcoolers, J. Appl. Phys. 95 (2004) 8226–8232.
[15] J. Cheng, C. Liu, Y. Chao, R. Tain, Cooling performance of silicon-based thermoelectric device on high power LED, in: International Conference on Thermoelectrics, ICT, Proceedings, 2005, IEEE, Piscataway, NJ, USA, 2005, pp. 53–56.
[16] M. Hodes, On one-dimensional analysis of thermoelectric modules (TEMs), IEEE Trans. Compon. Packag. Technol. 28 (2) (2005) 218–229.
[17] M. Huang, R. Yen, A. Wang, The influence of the Thomson effect on the performance of a thermoelectric cooler, Int. J. Heat Mass Transfer 48 (2005) 413–418.
[18] Y. Kraftmakher, Simple experiments with a thermoelectric module, Eur. J. Phys. 26 (2005) 959–967.
[19] K. Lee, O. Kim, Analysis on the cooling performance of the thermoelectric micro-cooler, Int. J. Heat Mass Transfer 50 (2007) 1982–1992.
[20] Y. Chang, C. Chang, M. Ke, S. Chen, Thermoelectric air-cooling module for electronic devices, Appl. Therm. Eng. 29 (2009) 2731–2737.
[21] O. Yamashita, Resultant Seebeck coefficient formulated by combining the Thomson Effect with the intrinsic Seebeck coefficient of a thermoelectric element, Energy Convers. Manage. 50 (2009) 2394–2399.
[22] P. Pichanusakorn, P.R. Bandaru, The optimal Seebeck coefficient for obtaining the maximum power factor in thermoelectrics, Appl. Phys. Lett. 94 (22) (2009) 223108-1–223108-3.